Reactions of $MH(OTf)(NBD)(PPh_3)_2$ (M = Ru, Os) with H_2

Shu Tak Lo,[†] Zhitao Xu,[†] Ting Bin Wen,[†] Weng Sang Ng,[†] Sheng Hua Liu,[†] Zhong Yuan Zhou,[‡] Zhenyang Lin,*[,†] Chak Po Lau,*[,‡] and Guochen Jia*[,†]

Department of Chemistry, The Hong Kong University of Science and Technology, Clear Water Bay, Kowloon, Hong Kong, and Department of Applied Biology & Chemical Technology, The Hong Kong Polytechnic University, Hung Hom, Kowloon, Hong Kong

Received May 1, 2000

Treatment of $RuHCl(NBD)(PPh_3)_2$ (NBD = norbornadiene) with AgOTf produced $RuH(OTf)(NBD)(PPh_3)_2$. Reaction of $RuH(OTf)(NBD)(PPh_3)_2$ with H_2 in benzene gave norbornene and $[(\eta^6\text{-}C_6H_6)RuH(PPh_3)_2]OTf$. The same reaction in CD_2Cl_2 in the presence of added PPh_3 produced norbornane and $[RuH(PPh_3)_4]OTf$. Reaction of $OsH_3Cl(PPh_3)_3$ with norbornadiene produced $OsHCl(NBD)(PPh_3)_2$, which was converted to $OsH(OTf)(NBD)(PPh_3)_2$ on treatment with AgOTf. Reaction of $OsH(OTf)(NBD)(PPh_3)_2$ with H_2 in benzene gave norbornane and $[(\eta^6\text{-}C_6H_6)OsH(PPh_3)_2]OTf$. In dichloromethane, $OsH(OTf)(NBD)(PPh_3)_2$ reacted with H_2 in the presence of added PPh_3 to produce norbornane and $[OsH_3(PPh_3)_4]OTf$. Supported by computational studies, it is assumed that the dihydrogen complexes $[MH(H_2)(NBD)(PPh_3)_2]^+$ (M = Ru, Os) were involved in the hydrogenation reactions. Two reaction pathways for the conversion of $[RuH(H_2)(NBD)(PH_3)_2]^+$ to $[RuH(NBE)(PH_3)_2]^+$ (NBE = norbornene) have been studied by density functional theory calculations. The results show that the first hydrogen transferred to the olefin ligand is more likely from the hydride ligand rather than from the dihydrogen ligand.

Introduction

Since the first report of dihydrogen complexes in 1984,[1] this unique class of complexes have been intensively investigated, especially their preparation, characterization, and structural and catalytic properties.[2] A relatively less studied aspect of the chemistry of dihydrogen complexes is their reactivities toward organic ligands (e.g., alkyls, vinyls, vinylidenes, and olefins), although such study should help to clarify the mechanisms of reactions mediated by dihydrogen complexes and to further develop new catalytic reactions based on dihydrogen complexes. It has been shown that a coordinated dihydrogen ligand in $L_nM(H_2)R$ could transfer one of the hydrogen atoms of the dihydrogen ligand to the α-carbons of alkyl or vinyl ligands R to form L_nMH and RH. Such a reactivity has been invoked to explain the catalytic activity of $RuHCl(PPh_3)_3$[3] and $[MH(H_2)(PP_3)]^+$ (M = Fe, Ru; $PP_3 = P(CH_2CH_2PPh_2)_3$)[4] for hydrogenation of olefins and acetylenes. The reactions are also thought to be involved in the reactions of some d^0 alkyl complexes with H_2 to give hydride complexes and alkanes.[5] Alkynyl−dihydrogen complexes have been reported for $[Ru(H_2)(C{\equiv}CPh)(dippe)_2]BPh_4$[6a] and $OsH(H_2)(C{\equiv}CPh)(CO)(P(i\text{-}Pr)_3)_2$.[6b] Hydrogen transfer from H_2 to the β-carbon of vinylidene ligands has been proposed for the reactions of $OsH_2Cl_2(P(i\text{-}Pr)_3)_2$ with $HC{\equiv}CR$ to give the carbyne complex $OsHCl_2(\equiv CCH_2R)(P(i\text{-}Pr)_3)_2$ via the intermediates $OsCl_2(H_2)(C{=}CHR)(P(i\text{-}Pr)_3)_2$.[7]

Oxidative coupling reactions of coordinated olefins and acetylenes are among the most common organometallic reactions.[8] In principle, a coordinated dihydrogen ligand may also undergo oxidative coupling reactions with unsaturated substrates such as olefins and acetylenes. However, examples of these reactions or even olefin−dihydrogen complexes are still very rare. Coupling between H_2 and olefin ligands has been proposed in the catalytic hydrogenation of olefins using $M(CO)_6$ (M = Cr, Mo, and W)[9] and $[TpRu(PPh_3)_x(CH_3CN)_{3-x}]^+$ ($x = 1, 2$)[10] and in the protonation reaction of Cp*RuH(NBD).[11] Reported olefin−dihydrogen complexes are limited to $M(H_2)(\eta^4\text{-}NBD)(CO)_3$ (M = Cr, Mo, and W) and $M(H_2)(\eta^2\text{-}NBD)(CO)_4$ (M = Mo and W), which have been detected by IR spectroscopy,[9] and $[Cp^*Ru(H_2)(COD)]^+$, which has been detected by NMR spectroscopy.[11]

[†] The Hong Kong University of Science and Technology.
[‡] The Hong Kong Polytechnic University.

(1) Kubas, G. J.; Ryan, R. R.; Swanson, B. I.; Vergamini, P. J.; Wasserman, H. J. *J. Am. Chem. Soc.* **1984**, *106*, 451.
(2) (a) Crabtree, R. H. *Angew. Chem., Int. Ed. Engl.* **1993**, *32*, 789. (b) Heinekey, D. M.; Oldham, W. J., Jr. *Chem. Rev.* **1993**, *93*, 913. (c) Jessop, P. G.; Morris, R. H. *Coord. Chem. Rev.* **1992**, *121*, 155. (d) Esteruelas, M. A.; Oro, L. A. *Chem. Rev.* **1998**, *98*, 577.
(3) Crabtree, R. H. *The Organometallic Chemistry of the Transition Metals*, 2nd ed.; John Wiley & Sons: New York, 1994; p 221.
(4) Bianchini, C.; Meli, A.; Peruzzini, M.; Frediani, P.; Bohanna, C.; Esteruelas, M. A.; Oro, L. A. *Organometallics* **1992**, *11*, 138.
(5) Ziegler, T.; Folga, E.; Berces, A. *J. Am. Chem. Soc.* **1993**, *115*, 636, and references therein.
(6) (a) Tenorio, M. J.; Puerta, M. C.; Valerga, P. *J. Chem. Soc., Chem. Commun.* **1993**, 1750. (b) Espuelas, J.; Esteruelas, M. A.; Lahoz, F. J.; Oro, L. A.; Valero, C. *J. Am. Chem. Soc.* **1993**, *115*, 4683.
(7) Espuelas, J.; Esteruelas, M. A.; Lahoz, F. J.; Oro, L. A.; Ruiz, N. *J. Am. Chem. Soc.* **1993**, *115*, 4683.
(8) Crabtree, R. H. *The Organometallic Chemistry of the Transition Metals*, 2nd ed.; John Wiley & Sons: New York, 1994; pp155−158.
(9) (a) Jackson, S. A.; Hodges, P. M.; Poliakoff, M.; Turner, J. J.; Grevels, F. W. *J. Am. Chem. Soc.* **1990**, *112*, 1221. (b) Thomas, A.; Haake, M.; Grevels, F. W.; Bargon, J. *Angew. Chem., Int. Ed. Engl.* **1994**, *33*, 755.
(10) Chan, W. C.; Lau, C. P.; Chen, Y. Z.; Fang, Y. Q.; Ng, S. M.; Jia, G. *Organometallics* **1997**, *16*, 34.
(11) Jia, G.; Ng, W. S.; Lau, C. P. *Organometallics* **1998**, *17*, 4538.

10.1021/om000369x CCC: $19.00
Publication on Web 09/27/2000

Scheme 1

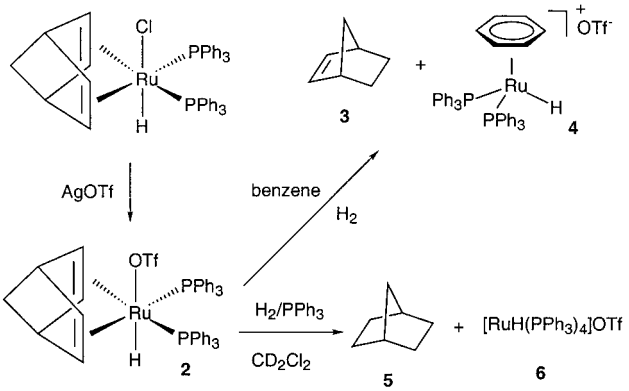

To further model reactions of coordinated dihydrogen ligand with olefin and alkyl ligands, we have investigated the reactions of hydrogen with MH(OTf)(NBD)$(PPh_3)_2$ (M = Ru, Os). As triflate has been recognized as a facile leaving group that can be readily displaced under mild conditions[12] and a number of dihydrogen complexes of the type $[MH(H_2)(L_4)]^+$ (M = Ru, Os; L_4 = mono- to tetradentate phosphorus ligands) have previously been well characterized,[13] one might expect that reactions of H_2 with MH(OTf)(NBD)$(PPh_3)_2$ (M = Ru, Os) may produce the dihydrogen complexes $[MH(H_2)$-$(NBD)(PPh_3)_2]^+$. The latter dihydrogen complexes may undergo hydrogen transfer reactions to hydrogenate the NBD ligand. Complexes $[MH(H_2)(NBD)(PPh_3)_2]^+$ are interesting because both η^2-H_2 and hydride ligands are present on the same metal center having an olefin moiety. Thus this provides a good opportunity to study whether hydrogen transfer from the η^2-H_2 or the hydride ligand to the olefin ligand is easier.

Results and Discussion

Preparation of RuH(OTf)(NBD)$(PPh_3)_2$. The complex RuH(OTf)(NBD)$(PPh_3)_2$ (**2**) was prepared by treating RuHCl(NBD)$(PPh_3)_2$ (**1**) with AgOTf (Scheme 1). In the ^{1}H NMR spectrum in CD_2Cl_2, the CH_2 protons of the NBD exhibited a singlet at 0.89 ppm and the bridgehead protons of NBD displayed two signals at 2.98 and 4.35 ppm. The NMR data suggest that the hydride is trans to the OTf ligand and that the two PPh_3 ligands are cis to each other. A similar structure has been previously proposed for RuHCl(NBD)$(PPh_3)_2$.[14]

Scheme 2

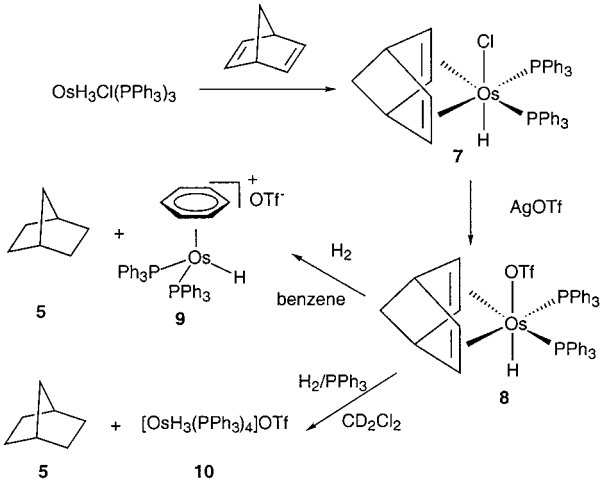

Reaction of H_2 with RuH(OTf)(NBD)$(PPh_3)_2$. Complex **2** in benzene reacted with H_2 to give norbornene (**3**) and the known hydride complex [(η^6-C_6H_6)-$RuH(PPh_3)_2]OTf$ (**4**).[15−17] As triflate is a good leaving group, the hydrogenation reaction is likely initiated by formation of the dihydrogen complex $[RuH(H_2)(NBD)$-$(PPh_3)_2]^+$ through displacement of the triflate anion with a H_2 molecule. To detect the intermediate, we have carried out the hydrogenation in dichloromethane at low temperature. It was shown that complex **2** in CD_2Cl_2 reacted with H_2 to give norbornane (**5**) and a mixture of phosphorus-containing species, which proved to be difficult to purify and characterize. In the presence of added PPh_3, complex **2** reacted with H_2 to give norbornane (**5**) and $[RuH(PPh_3)_4]OTf$[18] (**6**) (Scheme 1). We have not been able to detect the dihydrogen intermediate even when the reactions were carried out at low temperature.

Preparation of OsH(OTf)(NBD)$(PPh_3)_2$. For analogous dihydrogen complexes, osmium analogues are usually thermally more stable than their ruthenium counterparts.[2] Thus we have prepared the analogous complex OsH(OTf)(NBD)$(PPh_3)_2$, hoping that its subsequent reaction with H_2 would give the observable dihydrogen complex $[OsH(H_2)(NBD)(PPh_3)_2]^+$.

The synthetic route to the new osmium complex OsH-(OTf)(NBD)$(PPh_3)_2$ (**8**) is outlined in Scheme 2. Reaction of $OsH_3Cl(PPh_3)_3$[19] with NBD led to the formation of OsHCl(NBD)$(PPh_3)_2$ (**7**). The procedure is similar to that used to prepare RuHCl(NBD)$(PPh_3)_2$.[20] Complex **8** was then obtained in high yield by treating **7** with AgOTf.

Complex **7** has been characterized by NMR spectroscopy as well as elemental analysis. In particular, the ^{31}P NMR spectrum in CD_2Cl_2 showed a singlet at −12.1 ppm, indicating that the two PPh_3's are equivalent. In the ^{1}H NMR spectrum in CD_2Cl_2, five NBD proton signals were observed: the olefinic protons displayed

(12) Beck, W.; Sünkel, K. *Chem. Rev.* **1988**, *88*, 1405.
(13) See for example: (a) Schlaf, M.; Lough, A. J.; Morris, R. H. *Organometallics* **1997**, *16*, 1253. (b) Bianchini, C.; Masi, D.; Peruzzini, M.; Casarin, M.; Maccato, C.; Rizzi, G. A. *Inorg. Chem.* **1997**, *36*, 1061. (c) Ayllón, J. A.; Gervaux, C.; Sabo-Etienne, S.; Chaudret, B. *Organometallics* **1997**, *16*, 2000. (d) Rocchini, E.; Mezzetti, A.; Rüegger, H.; Burckhardt, U.; Gramlich, V.; Del Zotto, A.; Martinuzzi, P.; Rigo, P. *Inorg. Chem.* **1997**, *36*, 711. (e) Gusev, D. G.; Hübener, R.; Orama, O.; Berke, H. *J. Am. Chem. Soc.* **1997**, *117*, 3716, and references therein. (f) Albertin, G.; Antoniutti, S.; Baldan, D. Bordgnon, E. *Inorg. Chem.* **1995**, *34*, 6205. (g) Cappellani, E. P.; Drouin, S. D.; Jia, G.; Maltby, P. A.; Morris, R. H.; Schweitzer, C. T. *J. Am. Chem. Soc.* **1994**, *116*, 3375. (h) Field, L. D.; Hambley, T. W.; Yau, B. C. K. *Inorg. Chem.* **1994**, *33*, 2009. (i) Jia, G.; Drouin, S. D.; Jessop, P. G.; Lough, A. J.; Morris, R. H. *Organometallics* **1993**, *12*, 906. (j) Bianchini, C.; Linn, K. Masi, D. Peruzzini, M.; Polo, A.; Vacca, A.; Zanobini, F. *Inorg. Chem.* **1993**, *32*, 2366. (k) Michos, D.; Luo, X. L.; Crabtree, R. H. *Inorg. Chem.* **1992**, *31*, 4245. (l) Bianchini, C.; Perez, P. J.; Peruzzini, M.; Zanoboni, F.; Vacca, A. *Inorg. Chem.* **1991**, *30*, 279. (m) Earl, K. A.; Jia, G.; Maltby, P. A.; Morris, R. H. *J. Am. Chem. Soc.* **1991**, *113*, 3027. (m) Bautista, M. T.; Cappellani, E. P.; Drouin, S. D.; Morris, R. H.; Schweitzer, C. T.; Sella, A.; Zubkowski, J. *J. Am. Chem. Soc.* **1991**, *113*, 4876. (n) Amendola, P.; Antoniutti, S.; Albertin, G.; Bordignon, E. *Inorg. Chem.* **1990**, *29*, 318.
(14) Dekleva, T. W.; James, B. R. *J. Chem. Soc., Chem. Commun.* **1983**, 1350.
(15) Harding, P. A.; Robinson, S. D. *J. Chem. Soc., Dalton Trans.* **1988**, 415.
(16) Werner, R.; Werner, H. *Chem. Ber.* **1982**, *115*, 3781.
(17) Cole-Hamilton, D. J.; Young, R. J.; Wilkinson, G. *J. Chem. Soc., Dalton Trans.* **1976**, 1995.
(18) Sanders, J. R. *J. Chem. Soc., Dalton Trans.* **1973**, 743.
(19) Ferrando, G.; Caulton, K. G. *Inorg. Chem.* **1999**, *38*, 4168.
(20) Hallman, P. S.; McGarvey, B. R.; Wilkinson, G. *J. Chem. Soc. (A)* **1968**, 3143.

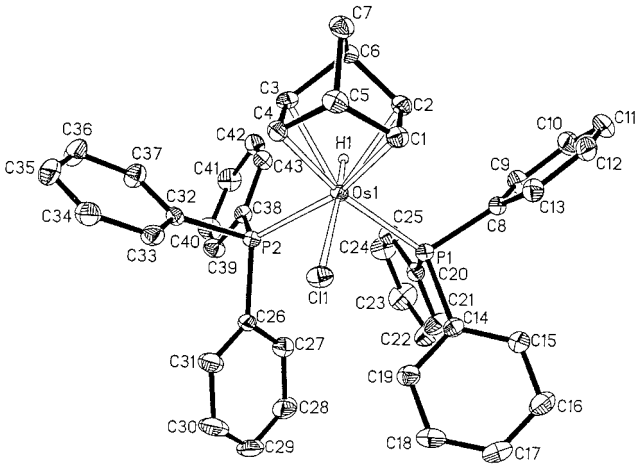

Figure 1. Molecular structure for OsHCl(NBD)(PPh$_3$)$_2$ showing 40% probability of thermal ellipsoids

Table 1. Crystal Data and Refinement Details for OsHCl(NBD)(PPh$_3$)$_2$

formula	$C_{43}H_{39}ClP_2Os$
fw	843.33
cryst syst	monoclinic
space group	$P2_1/n$
a, Å	12.9154(11)
b, Å	18.0172(15)
c, Å	15.3078(13)
β, deg	100.854(2)
V, Å^3	3498.4(5)
Z	4
d_{calc}, g cm^{-3}	1.601
abs coeff, mm^{-1}	3.844
radiation, Mo Kα, Å	0.71073
θ range, deg	1.76−27.51
no. of reflns collected	23 217
no. of ind reflns	8026 (R_{int} = 6.14%)
no. of obsd reflns	6509 ($I > 2\sigma(I)$)
no. of params refined	456
final R indices (obsd data)	R1 = 3.42%, wR2 = 8.09%
goodness of fit	0.972
largest diff peak, e Å^{-3}	2.253
largest diff hole, e Å^{-3}	−0.826

two signals at 3.02 and 3.22 ppm; the bridge-head protons also displayed two signals at 3.48 and 4.11 ppm; the CH_2 protons showed only one signal at 0.69 ppm. The pattern of the NBD ^{1}H signals implies that the two PPh_3 ligands are cis to each other and that the hydride is trans to the chloride.

The structure of **7** has been confirmed by an X-ray diffraction study. The molecular geometry of **7** is depicted in Figure 1. The crystallographic details and selected bond distances and angles are given in Tables 1 and 2, respectively. The structure of **7** can be viewed as a distorted octahedron in which two vertexes are occupied by the double bonds of the norbornadiene ligand. The two PPh_3 ligands are cis to each other, although P(1)−Os(1)−P(2) angle (101.21(2)°) is significantly distorted from 90°. The norbornadiene ligand is symmetrically coordinated to osmium with the double bonds trans to the PPh_3 ligands. The C═C bonds of norbornadiene are significantly lengthened relative to free NBD, and the C═C bond distances are similar to those observed in $RuCl_2(NBD)(PPh_3)_2$.[21] The Os−C bond distances are close to those observed in osmium olefin complexes such as $OsCl_2(\eta^4\text{-COD})(\eta^2\text{-}CH_2{=}CMeP(i\text{-}Pr)_2)$[22] and $OsCl_2(\eta^4\text{-TFB})(\eta^2\text{-}CH_2{=}CMeP(i\text{-}Pr)_2)$ (TFB = tetrafluorobenzobarrelene).[22]

As indicated by its NMR spectroscopic data, complex **8** must have a geometry similar to that of complex **7**. Reported complexes closely related to **7** and **8** are the osmium dihydrido diolefin complexes $OsH_2(\eta^4\text{-diolefin})(P(i\text{-}Pr)_3)_2$ (diolefin = COD, NBD, TFB).[23] Unlike complexes **7** and **8**, the two phosphine ligands are trans to each other in $OsH_2(\eta^4\text{-diolefin})(P(i\text{-}Pr)_3)_2$.

Reaction of H$_2$ with OsH(OTf)(NBD)(PPh$_3$)$_2$. Complex **8** in benzene reacted with H_2 to give norbornane (**5**) and the known hydride complex $[\eta^6\text{-}C_6H_6)OsH(PPh_3)_2]OTf$ (**9**)[17] (see Scheme 2). On the contrary, ruthenium complex **2** reacted with H_2 in benzene to give norbornene. In CD_2Cl_2 at room temperature, complex **8** reacted with H_2 to give norbornane and a mixture of uncharacterized phosphorus-containing species. If complex **8** in CD_2Cl_2 was allowed to react with H_2 at low temperature, a mixture of unstable hydride species was produced as indicated by ^{1}H NMR. However, the expected hydride complex $[OsH(H_2)(NBD)(PPh_3)_2]^+$ or $[OsH_3(NBD)(PPh_3)_2]^+$ could not be identified. In the presence of added PPh_3, complex **8** reacted with H_2 to give to norbornane and $[OsH_3(PPh_3)_4]^+$ (**10**).[24]

Comments on the Possible Mechanisms for the Hydrogenation of NBD. As triflate can be displaced easily, it is reasonable to assume that the first step of the reaction is to displace the triflate anion in MH(OTf)(NBD)(PPh$_3$)$_2$ with a H_2 molecule to give dihydrogen complexes $[MH(H_2)(NBD)(PPh_3)_2]^+$ (**11**) or the hydride complexes $[MH_3(NBD)(PPh_3)_2]^+$ (M = Ru, Os). We favor the formulation of dihydrogen complexes, as a number of complexes of the type $[MH(H_2)(L_4)]^+$ (M = Ru, Os; L = phosphines) have previously been well characterized and as NBD is a better π acceptor than phosphines. Once the dihydrogen complexes were formed, the NBD can be hydrogenated by transfer of a hydrogen atom either from the hydride or the dihydrogen ligand to the olefin ligand followed by transfer of the second one to give norbornene. Insertions of olefins to M−H bonds and hydrogen transfer from the η^2-H_2 ligand to coordinated olefins are all known reactions. The norbornane is presumably formed by further hydrogenation of norbornene. We noted that the NBD ligand in RuH(OTf)(NBD)(PPh$_3$)$_2$ in benzene is hydrogenated to norbornene, but that in OsH(OTf)(NBD)(PPh$_3$)$_2$ in benzene is hydrogenated to norbornane. The difference could be attributed to the stronger bonding of NBE to osmium relative to ruthenium.

Structures of $[MH(H_2)(NBD)(PH_3)_2]^+$ (M = Ru, Os). Although dihydrogen complexes $[MH(H_2)(NBD)(PPh_3)_2]^+$ (M = Ru, Os) are the likely intermediates for the reactions of MH(OTf)(NBD)(PPh$_3$)$_2$ with H_2, we have not been able to characterize them experimentally. Thus a computational study was carried out in order to see if the dihydrogen complexes are reasonable species. To find out the ground-state structures of $[MH(H_2)(NBD)(PPh_3)_2]^+$, density functional calculations have been carried out for the model complexes $[MH(H_2)(NBD)(PH_3)_2]^+$. The optimization on the structure of [RuH-

(21) Bergbreiter, D. E.; Bursten, B. E.; Bursten, M. S.; Cotton, F. A. *J. Organomet. Chem.* **1981**, *205*, 407.
(22) Edwards. A. J.; Esteruelas, M. A.; Lahoz, F. J.; López, A. M.; Oñate, E.; Oro, L. A.; Tolosa, J. I. *Organometallics* **1997**, *16*, 1316.
(23) Castillo, A.; Esteruelas, M. A.; Oñate, E.; Ruiz, N. *J. Am. Chem. Soc.* **1997**, *119*, 9691.
(24) Siedle, A. R.; Newmark, R. A.; Pignolet, L. H. *Inorg. Chem.* **1986**, *25*, 3412.

Table 2. Selected Bond Distances and Angles for $OsHCl(NBD)(PPh_3)_2$

Bond Distances (Å)

Os(1)−P(1)	2.3918(11)	Os(1)−P(2)	2.3739(10)	Os(1)−Cl(1)	2.4997(10)
Os(1)−C(1)	2.211(4)	Os(1)−C(2)	2.206(4)	Os(1)−C(3)	2.209(4)
Os(1)−C(4)	2.203(4)	C(1)−C(2)	1.410(6)	C(3)−C(4)	1.397(6)
C(1)−C(5)	1.543(6)	C(2)−C(6)	1.529(6)	C(3)−C(6)	1.531(6)
C(4)−C(5)	1.546(6)	C(5)−C(7)	1.553(6)	C(6)−C(7)	1.539(6)
Os(1)−H(1)	1.727				

Bond Angles (deg)

P(1)−Os(1)−P(2)	101.18(4)	P(1)−Os(1)−Cl(1)	91.94(4)
P(1)−Os(1)−C(1)	98.75(12)	P(1)−Os(1)−C(2)	93.83(12)
P(1)−Os(1)−C(3)	148.97(11)	P(1)−Os(1)−C(4)	162.12(12)
P(2)−Os(1)−Cl(1)	87.40(4)	P(2)−Os(1)−C(1)	158.17(12)
P(2)−Os(1)−C(2)	148.17(12)	P(2)−Os(1)−C(3)	90.60(12)
P(2)−Os(1)−C(4)	94.91(12)	Cl(1)−Os(1)−C(1)	83.11(11)
Cl(1)−Os(1)−C(2)	120.23(11)	Cl(1)−Os(1)−C(3)	117.42(11)
Cl(1)−Os(1)−C(4)	80.97(11)	C(1)−Os(1)−C(2)	37.23(15)
C(1)−Os(1)−C(3)	76.59(16)	C(1)−Os(1)−C(4)	64.25(17)
C(2)−Os(1)−C(3)	63.68(6)	C(2)−Os(1)−C(4)	76.02(16)
C(3)−Os(1)−C(4)	36.93(15)		

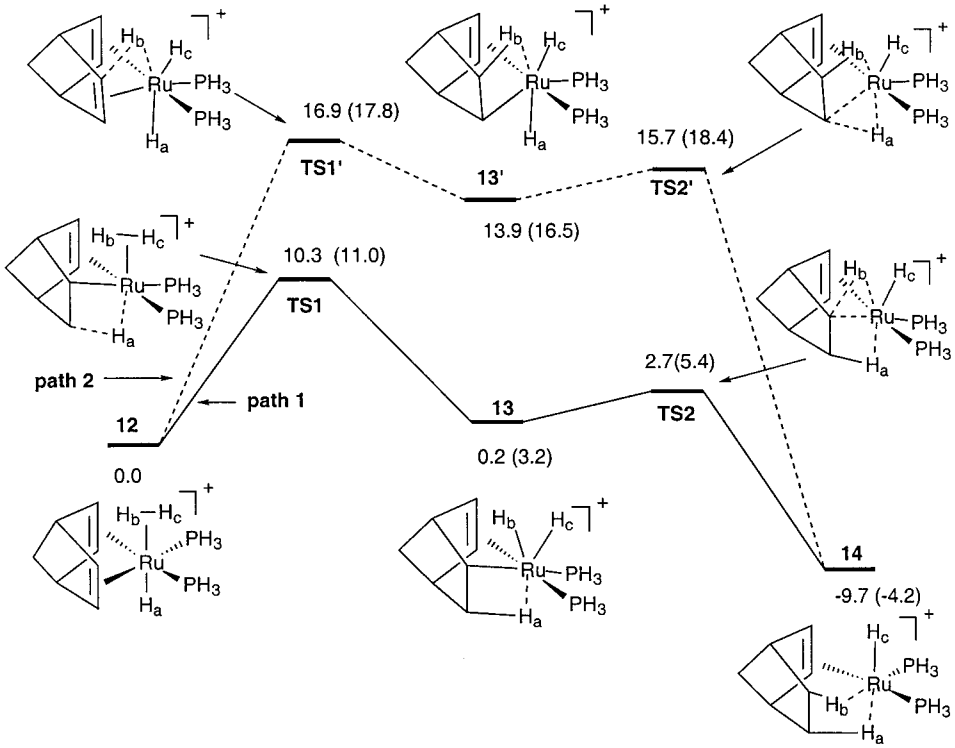

Figure 2. Schematic illustration of the two reaction pathways together with calculated relative energies (kcal/mol) and free energies (kcal/mol, in parentheses) for species involved in the reaction

$(H_2)(NBD)(PH_3)_2]^+$ (**12**) shows that complex **12** is indeed a typical dihydrogen complex in which the nonclassical η^2-H_2 ligand is trans to the hydride ligand and has a short H−H distance of 0.793 Å (see discussion in the next section). As expected, the distances between Ru and the two hydrogen atoms of the dihydrogen ligand are much longer (∼1.95 Å) than that between Ru and the terminal hydride ligand (1.595 Å). A similar optimized structure was obtained for $[OsH(H_2)(NBD)(PH_3)_2]^+$, in which the two hydrogen atoms of the dihydrogen ligand are separated by 0.831 Å. It should be noted that the related complex $[OsH_3(NBD)(P(i\text{-}Pr)_3)_2]^+$ is known to adopt a trihydride structure.[23] However, the complex is different from ours in that the phosphine is more electron donating and the two sterically more demanding phosphines prefer to be trans to each other.

Theoretical Study on the Reaction Pathways of the Conversion of $[RuH(H_2)(NBD)(PH_3)_2]^+$ to $[RuH(NBE)(PH_3)_2]^+$. As mentioned previously, hydrogenation of the NBD ligand in $[MH(H_2)(NBD)(PPh_3)_2]^+$ can be initiated by transfer of a hydrogen to the olefin ligand from either the hydride or the dihydrogen ligand. To clarify whether hydrogen transfer from the η^2-H_2 or the hydride ligand to the olefin ligand in $[MH(H_2)(NBD)(PPh_3)_2]^+$ is more likely the first step for the hydrogenation reactions, density functional theory calculations have been carried out for all stable and transition structures for the two reaction pathways involved in the conversion of the model complex $[RuH(H_2)(NBD)(PH_3)_2]^+$ to $[RuH(NBE)(PH_3)_2]^+$ (NBE = norbornene).

Figure 2 shows the two possible reaction pathways studied here for the conversion of $[RuH(H_2)(NBD)$-

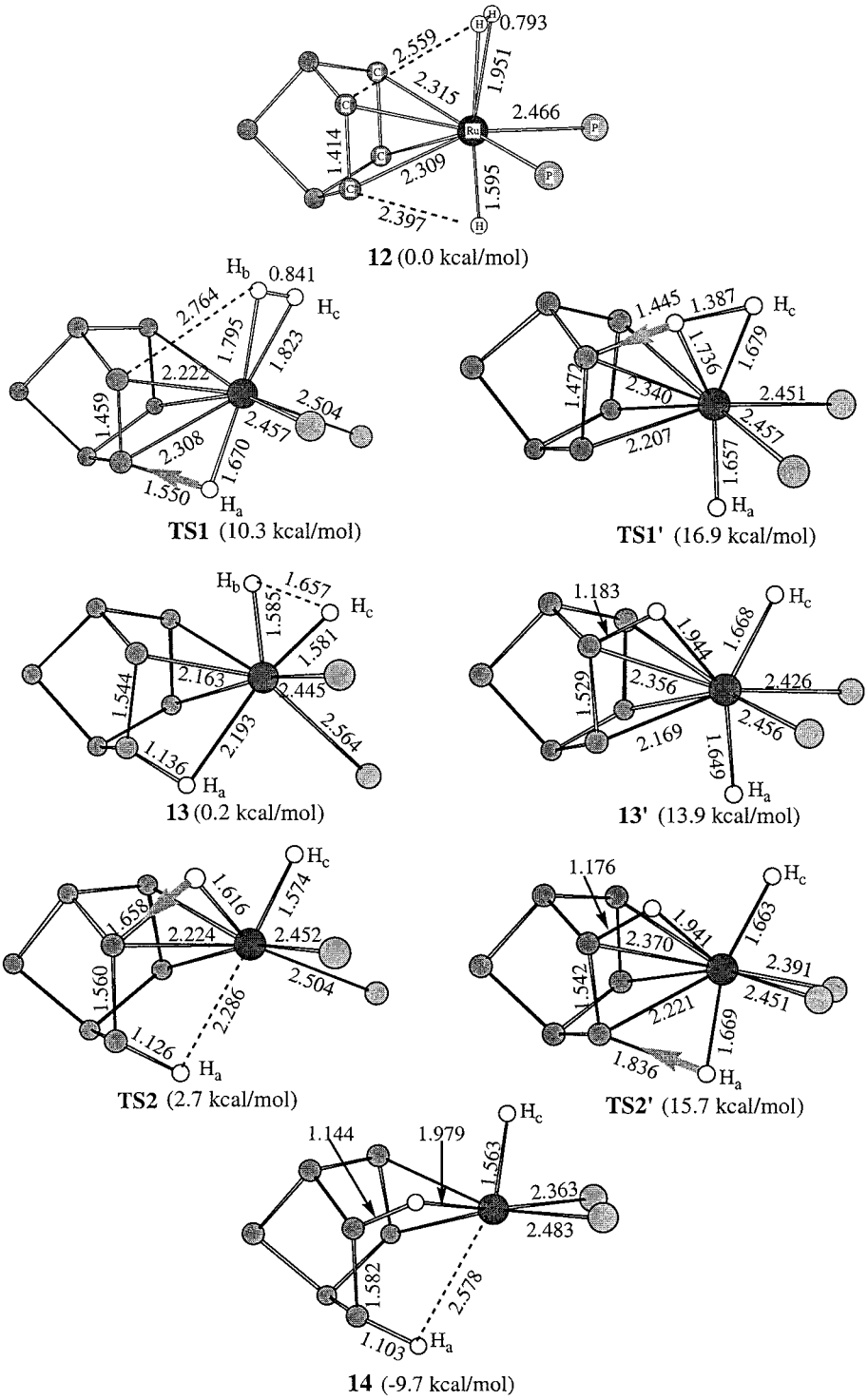

Figure 3. Optimized structures with selected geometry parameters (and relative stability). The hydrogen atoms, which are not directly involved in the hydrogenation, have been omitted for the purpose of clarity

$(PH_3)_2]^+$ to $[RuH(NBE)(PH_3)_2]^+$.[25] Path 1 starts with the hydrogen transfer from the hydride ligand (H_a) followed by the cleavage of the dihydrogen ligand to form a cis dihydride intermediate **13**; then the second hydrogen transfers from one (H_b) of the two hydride ligands to complete the hydrogenation and gives a coordinated NBE complex **14**. By contrast, the second pathway (path 2) starts with the first hydrogen transfer from the dihydrogen ligand (H_b) to form a trans (or nearly trans) dihydride intermediate **13′**; the second hydrogen transfers from the original hydride ligand (H_a) to form the same norbornene (NBE) complex **14** as in path 1.

Figure 2 also shows the relative reaction energies and free energies (in brackets) calculated for all the species (stable and transition structures). It is clear that the relative free energies do not differ too much from the relative reaction energies. These results suggest that the entropy contribution is not important because the reaction paths involve only structural rearrangement

(25) Another possible pathway is the concert hydrogen transfer from both hydride and dihydrogen ligands. However, we were not able to locate the transition state in our calculations.

within the molecules. Therefore, we will use the reaction energies for discussion since the differences between the reaction energies and free energies are small.

For both reaction pathways, the reaction barriers of the first hydrogen transfer (10.3 and 16.9 kcal/mol) are much higher than those of the second hydrogen transfer (2.5 and 1.8 kcal/mol), indicating that the first hydrogen transfer is the rate-determining step. Overall, the reaction barriers of path 1 are significantly lower than those of path 2, suggesting that path 1 is the main channel of the hydrogenation of NBD in this Ru complex. The low activation energy (10.3 kcal/mol) of path 1 is in agreement with the experimental observation that the NBD ligand is hydrogenated rapidly and that the dihydrogen complex $[RuH(H_2)(NBD)(PPh_3)_2]^+$ could not be observed.

One may ask why the overall activation energy of path 1 is significantly lower than that of path 2, and why the reaction barriers for the first hydrogen transfer of both pathways are much higher than those of the second hydrogen transfer. To answer these questions, the calculated geometries of the related structures are examined below.

Figure 3 shows the optimized structures with selected structural parameters for all related species. The reactant (**12**) is a typical dihydrogen complex in which the nonclassical η^2-H_2 ligand is trans to the hydride ligand (H_a) and has a short H_b-H_c distance of 0.793 Å. The first transition state (**TS1**) of path 1 is also a nonclassical complex with a slightly longer H_b-H_c distance (0.841 Å). However, the first transition state (**TS1′**) of path 2 has a much longer H_b-H_c distance (1.387 Å) and typical Ru−hydride distances (see Figure 3 for details), especially $Ru-H_a$ and $Ru-H_c$. The short Ru−H distances suggest that **TS1′** could be considered as a trihydride with two hydride ligands (H_a and H_c) trans (or nearly trans) to each other. The high relative energy of this trihydride structure, compared with that of **TS1**, reveals that the strong trans influence between H_a and H_c (or H_b) plays an important role in this transition state. The trans influence of a hydride ligand weakens the metal−ligand interaction at the position trans to it and thus destabilizes the system.[26]

As the first hydrogen moves closer to the olefin ligand, **TS1** gives a cis dihydride intermediate (**13**) with a weak agostic interaction between the Ru center and H_a while **TS1′** gives a trans dihydride intermediate (**13′**). The higher energy of **13′** is again due to the strong trans influence between H_a and H_c. This strong trans influence is also reflected by the relevant structural parameters that the Ru−H distances in **13′** ($Ru-H_a$ and $Ru-H_c$) are longer than those in **13** ($Ru-H_b$ and $Ru-H_c$). The second hydrogen transfer in path 1 gives a cis dihydride transition structure (**TS2**) while that in path 2 leads to a trans dihydride transition structure (**TS2′**). The higher relative energy of **TS2′** can be easily related to the trans influence between H_a and H_c.

It is obvious that the high relative energies of structures **TS1′**, **13′**, and **TS2′** are all related to the trans influence between the hydride ligands in these species. Such a trans influence also explains why the overall activation energies of path 2 are higher than those of path 1.

Now we come to the second question why the activation energies required for the first hydrogen transfer are much higher than those for the second hydrogen transfer for both reaction pathways. Carefully examination of the geometrical changes during the relevant hydrogen transfer steps provides helpful information to the understanding of this problem. The geometrical changes from the reactant to the first transition structures (**TS1** and **TS1′**) are quite significant. The $Ru-H_b/H_b-H_c$ distances change from 1.951/0.793 Å to 1.795/0.841 Å for path 1 and to 1.736/1.387 Å for path 2. These remarkable changes give rise to higher activation energies required for the first hydrogen transfers in both paths. However, **TS2** and **TS2′** are structurally similar to **13** and **13′**, respectively. The similarity leads to small changes in their stabilities and therefore the activation energies required for the second hydrogen transfers turn out to be much smaller.

Summary and Conclusions

The NBD ligand in $MH(OTf)(NBD)(PPh_3)_2$ (M = Ru, Os) is hydrogenated on treatment with H_2 gas. Formation of the dihydrogen complexes $[MH(H_2)(NBD)(PPh_3)_2]^+$ is likely the first event of the hydrogenation reactions, although the dihydrogen complexes could not be observed experimentally. Density functional calculations on the model complexes $[MH(H_2)(NBD)(PH_3)_2]^+$ confirm that $[MH(H_2)(NBD)(PH_3)_2]^+$ indeed adopts the dihydrogen form. Hydrogenation of the NBD ligand in $[MH(H_2)(NBD)(PPh_3)_2]^+$ can be initiated by first transfer of a hydrogen atom to the olefin ligand either from the hydride (path 1) or from the dihydrogen ligand (path 2). The density functional theory calculations at the BLYP level on the reaction pathways for the conversion of $[RuH(H_2)(NBD)(PH_3)_2]^+$ to $[RuH(H_2)(NBE)(PH_3)_2]^+$ found that the pathway (path 1) in which the first hydrogen transfer is from the hydride ligand has a lower reaction barrier than the other one (path 2) in which the first hydrogen transfer is from the dihydrogen ligand. The overall reaction barrier of path 1 is calculated to be low (the relative free energy is only 11.0 kcal/mol at room temperature). In good agreement with the experimental observations, this result indicates that the hydrogenation of NBD through the first reaction pathway (path 1) can go rapidly at room temperature. The higher reaction barrier of the second pathway is due to the trans influence of the trans dihydride transition states and intermediate involved. It is also found that the activation energies required for the first hydrogen transfer are much higher than that required for the second hydrogen transfer in both pathways. These differences in activation energies are related to the different degree of the geometry changes during the two steps of hydrogen transfers. The first hydrogen transfers in both pathways lead to significant geometry changes, especially for the Ru−H bond lengths, while the second hydrogen transfers do not cause remarkable geometry changes.

Experimental Section

All manipulations were carried out under a nitrogen atmosphere using standard Schlenk techniques. Solvents were

(26) (a) Lin, Z.; Hall, M. B. *J. Am. Chem. Soc.* **1992**, *114*, 6102. (b) Xu, Z.; Bytheway, I.; Jia, G.; Lin, Z. *Organometallics* **1999**, *18*, 1761.

distilled under nitrogen from sodium benzophenone (hexane, ether, THF) or sodium (benzene) or calcium hydride (CH_2Cl_2). The starting materials RuHCl(NBD)(PPh_3)$_2$,[20] $OsCl_2(PPh_3)_3$,[27] and $OsH_3Cl(PPh_3)_3$[19] were prepared according to literature methods. All other reagents were used as purchased from Aldrich Chemical Co.

Microanalyses were performed by M-H-W Laboratories (Phoenix, AZ). ^{1}H, ^{13}C{^{1}H}, and ^{31}P{^{1}H} NMR spectra were collected on a JEOL EX-400 spectrometer (400 MHz) or a Bruker ARX-300 spectrometer (300 MHz). ^{1}H and ^{13}C NMR chemical shifts are relative to TMS, and ^{31}P NMR chemical shifts are relative to 85% H_3PO_4. MS spectra were recorded on a Finnigan TSQ7000 spectrometer.

RuH(OTf)(NBD)(PPh_3)$_2$. A mixture of RuHCl(NBD)(PPh_3)$_2$ (1.25 g, 1.66 mmol) and AgOTf (0.60 g, 2.7 mmol) in THF (35 mL) was stirred for 0.5 h. The solvent was then removed completely under vacuum. Addition of 50 mL of 10% MeOH aqueous solution to the residue produced a yellow solid, which was collected by filtration, washed with water, and dried under vacuum for 3 h. The solid was then extracted with 8:1 benzene/hexane. The extraction was filtered through a column of Celite. The volume of the filtrate was reduced to ca. 1 mL under vacuum. A pale yellow solid was formed when 40 mL of hexane was added. The solid was collected on a filter frit, washed with hexane, and dried under vacuum. Yield: 0.94 g, 60%. Anal. Calcd for $C_{44}H_{39}F_3O_3P_2SRu$: C, 60.89; H, 4.53. Found: C, 60.75; H, 5.13. ^{1}H NMR (300.13 MHz, C_6D_6): δ −13.64 (t, J(PH) = 22.5 Hz, 1 H, RuH), 0.89 (s, 2 H, CH_2), 2.98 (s, 1 H, bridge-head CH), 3.61 (s, 2 H, olefinic protons), 4.35 (br s, 3 H, two olefinic protons and one bridge-head CH proton), 7.00−7.60 (m, 30 H, PPh_3). ^{31}P{^{1}H} NMR (121.49 MHz, C_6D_6): δ 41.5 (s).

OsHCl(NBD)(PPh_3)$_2$. A mixture of $OsH_3Cl(PPh_3)_3$ (1.32 g, 1.30 mmol) and NBD (1.0 mL, 9.3 mmol) in benzene (35 mL) was stirred for 8 h to give a brown solution, which was filtered through a column of Celite. The solvent of the filtrate was then removed completely under vacuum. Addition of hexane (30 mL) to the residue produced a brown solid. After stirring for 0.5 h, the solid was collected by filtration, washed with hexane, and dried under vacuum. Yield: 0.98 g, 89%. Anal. Calcd for $C_{43}H_{39}ClP_2Os$: C, 61.24; H, 4.66. Found: C, 61.34; H, 4.82. ^{1}H NMR (300.13 MHz, C_6D_6): δ −12.13 (t, J(PH) = 22.5 Hz, 1 H, OsH), 0.69 (s, 2 H, CH_2), 3.02 (d, J(HH) = 3.5 Hz, 2 H, olefinic CH protons), 3.22 (s, 2 H, olefinic CH protons), 3.48 (s, 1 H, bridge-head CH proton), 4.11 (s, 1 H, CH), 7.00−7.80 (m, 30 H, PPh_3). ^{31}P{^{1}H} NMR (121.49 MHz, C_6D_6): δ 2.8 (s). ^{13}C{^{1}H} NMR (75.47 MHz, C_6D_6): δ 41.0 (d, J(PC) = 4.6 Hz, olefinic CH), 45.1 (s, bridge-head CH), 47.4 (d, J(PC) = 15.9 Hz, olefinic CH), 49.2 (s, CH_2), 62.1 (t, J(PC) = 5.4 Hz, bridge-head CH), 127.0−134.7 (m, Ph).

OsH(OTf)(NBD)(PPh_3)$_2$. A mixture of OsHCl(NBD)(PPh_3)$_2$ (0.95 g, 1.1 mmol) and AgOTf (0.65 g, 2.95 mmol) in THF (25 mL) was stirred for 0.5 h. The solvent was then removed completely under vacuum. Addition of 50 mL of 10% MeOH aqueous solution to the residue produced a yellow solid, which was collected by filtration, washed with water, and dried under vacuum for 3 h. The solid was then extracted with 8:1 benzene/hexane. The extraction was filtered through a column of Celite. The volume of the filtrate was reduced to ca. 1 mL under vacuum. A pale yellow solid was formed when 40 mL of hexane was added. The solid was collected on a filter frit, washed with hexane, and dried under vacuum. Yield: 0.63 g, 61%. Anal. Calcd for $C_{44}H_{39}F_3O_3P_2SOs$: C, 55.22; H, 4.11. Found: C, 55.49; H, 5.25. ^{1}H NMR (300.13 MHz, C_6D_6): δ −17.57 (t, J(PH) = 21.0 Hz, 1 H, OsH), 0.68 (s, 2 H, CH_2), 3.26 (s, 1 H, bridge-head CH proton), 3.44 (s, 2 H, olefinic CH proton), 3.90 (d, J(HH) = 3.3 Hz, 2 H, olefinic CH proton), 4.73 (s, 1 H, bridge-head CH proton), 7.10−7.90 (m, 30 H, PPh_3). ^{31}P{^{1}H} NMR (121.49 MHz, C_6D_6): δ 12.5 (s).

(27) Hoffmann, P. R.; Caulton, K. G. *J. Am. Chem. Soc.* **1975**, *97*, 4221.

Reaction of RuH(OTf)(NBD)(PPh_3)$_2$ with H_2 in CD_2Cl_2 in the Presence of PPh_3. A mixture of RuH(OTf)(NBD)(PPh_3)$_2$ (20 mg, 0.023 mmol) and PPh_3 (30 mg, 0.11 mmol) in CD_2Cl_2 (0.7 mL) in an NMR tube was allowed to stand under H_2 atmosphere for 1 h. The mixture was occasionally shaken. Then ^{1}H and ^{31}P{^{1}H} NMR spectra were collected. ^{31}P{^{1}H} NMR (121.49 MHz, CD_2Cl_2): δ − 6.0 (s, free PPh$_3$), 28.3 (s, br, [RuH(PPh$_3$)$_4$](OTf)[18]). ^{1}H NMR (300.13 MHz, CD_2Cl_2): δ −8.00 (quintet, J(PH) = 20.4 Hz, [RuH (PPh_3)$_4$](OTf)[18]), 0.90−2.19 (m, norbornane), 6.77−7.90 (m, PPh_3). Using a residual solvent signal at 5.32 ppm as the internal standard, the yield of norbornane was determined to be 81%. The volatile portion of the reaction mixture can be separated by vacuum transfer. A ^{1}H NMR spectrum of the vacuum-transferred solution shows that norbornane is the only volatile organic product formed in the reaction.

Reaction of RuH(OTf)(NBD)(PPh_3)$_2$ with H_2 in Benzene. A solution of RuH(OTf)(NBD)(PPh_3)$_2$ (0.35 g, 0.40 mmol) in benzene (30 mL) was stirred under a H_2 atmosphere for 1 h. The volume of the reaction mixture was then reduced to ca. 1 mL. Addition of hexane (50 mL) to the residue produced a white solid. The solid was collected by filtration, washed with hexane, and dried under vacuum. The solid was identified to be [(η^6-C_6H_6)RuH(PPh_3)$_2$]OTf.[15−17] Yield: 0.31 g, 91%. ^{1}H NMR (300.13 MHz, acetone-d_6): δ −8.83 (t, J(PH) = 36.9 Hz, RuH), 5.93 (s, 6 H, C_6H_6), 7.46−7.85 (m, Ph). ^{31}P{^{1}H} NMR (121.49 MHz, C_6D_6): δ 51.0 (s).

Identification of NBE Formed from the Reaction of RuH(OTf)(NBD)(PPh_3)$_2$ with H_2 in C_6D_6. A C_6D_6 solution (1 mL, contains 0.03% v/v TMS) of RuH(OTf)(NBD)(PPh_3)$_2$ (50 mg, 0.023 mmol) was allowed to stand under a H_2 atmosphere for 0.5 h. The mixture was occasionally shaken. Then ^{1}H and ^{31}P{^{1}H) NMR spectra were collected. ^{31}P{^{1}H} NMR (121.49 MHz, C_6D_6): δ 51.0 (s, [(η^6-C_6D_6)RuH(PPh_3)$_2$]OTf)[15−17]). ^{1}H NMR (300.13 MHz, C_6D_6): δ 0.79−1.74 (m, 6 H, CH_2), 2.73 (s, 2 H, bridge-head proton), 5.93 (s, 2 H, olefinic CH proton), 6.89−7.48 (m, PPh_3). Using the TMS signal as the internal standard, the yield of norbornene was determined to be 90%. The volatile portion of the reaction mixture can be separated by vacuum transfer. A ^{1}H NMR spectrum of the vacuum-transferred solution shows that norbornene is the only volatile organic product formed in the reaction.

Reaction of OsH(OTf)(NBD)(PPh_3)$_2$ with H_2 in CD_2Cl_2 in the Presence of PPh_3. A mixture of OsH(OTf)(NBD)(PPh_3)$_2$ (20 mg, 0.021 mmol) and PPh_3 (0.30 mg, 0.11 mmol) in CD_2Cl_2 (0.7 mL) in an NMR tube was allowed to stand under a H_2 atmosphere for 1 h. The mixture was occasionally shaken. Then ^{1}H and ^{31}P{^{1}H} NMR spectra were collected. ^{31}P{^{1}H} NMR (121.49 MHz, CD_2Cl_2): δ −6.0 (s, free PPh$_3$), −0.8 (br, [OsH_3(PPh$_3$)$_4$](OTf)[24]). ^{1}H NMR (300.13 MHz, CD_2Cl_2): δ −9.83 (quintet, J(PH) = 19.6 Hz, [OsH_3(PPh_3)$_4$](OTf)[24]), 0.92−2.07 (m, norbornane), 6.71−7.41 (m, PPh_3). Using residual solvent proton signal at 5.32 ppm as the internal standard, the yield of norbornane was determined to be 90%. The volatile portion of the reaction mixture can be separated by vacuum transfer. A ^{1}H NMR spectrum of the vacuum-transferred solution shows that norbornane is the only volatile organic product formed in the reaction.

Reaction of OsH(OTf)(NBD)(PPh_3)$_2$ with H_2 in C_6D_6. A C_6D_6 solution (1 mL, contains 0.03% v/v TMS) of OsH(OTf)(NBD)(PPh_3)$_2$ (20 mg, 0.021 mmol) in an NMR tube was allowed to stand under a H_2 atmosphere for 30 min. The mixture was occasionally shaken. Then ^{1}H and ^{31}P{^{1}H) NMR spectra were collected. ^{31}P{^{1}H} NMR (121.49 MHz, C_6D_6): δ 6.1 (s, [(η^6-C_6D_6)OsH(PPh_3)$_2$]OTf)[17]). ^{1}H NMR (300.13 MHz, C_6D_6): δ −11.35 (t, J(PH) = 17.5 Hz, [(η^6-C_6D_6)OsH(PPh_3)$_2$]-OTf), 1.00−1.44 (m, 8 H, CH_2 of norbornane), 2.15 (s, 2 H, CH of norbornane), 6.80−7.43 (m, [(η^6-C_6D_6)OsH(PPh_3)$_2$]OTf)[17]). Using the TMS signal as the internal standard, the yield of norbornane was determined to be 91%. The volatile portion of the reaction mixture can be separated by vacuum transfer. A

^{1}H NMR spectrum of the vacuum-transferred solution shows that norbornane is the only volatile organic product formed in the reaction. Pure samples of $[(\eta^6\text{-}C_6H_6)OsH(PPh_3)_2]OTf$ can be obtained on preparative scale from the reaction of $OsH(OTf)(NBD)(PPh_3)_2$ in C_6H_6 with H_2.

Crystallographic Analysis for $OsHCl(NBD)(PPh_3)_2$. Suitable crystals of $OsHCl(NBD)(PPh_3)_2$ for X-ray diffraction study were grown by layering of hexane on a CH_2Cl_2 solution of **7**. A brown prismatic single crystal having approximate dimensions of 0.12 × 0.10 × 0.06 mm was mounted in a glass fiber and used for X-ray structure determination. Intensity data were collected on a Bruker SMART CCD area detector using graphite-monochromated Mo Kα radiation ($\lambda = 0.71073$ Å). The intensity data were corrected for SADABS (Siemens area detector absorption[28]) (from 0.6555 to 0.8022 on I). The structure was solved by direct methods and refined by full-matrix least-squares analysis on F^2 using the SHELXTL (version 5.10) program package.[29] All non-hydrogen atoms were refined anisotropically. The H atoms of the phenyl rings of the PPh_3 ligands were introduced at calculated positions and refined via a riding model. The H atoms of the NBD were located from the difference Fourier map and refined with isotropic thermal parameters. The metal-bound hydrido ligand could be located satisfactorily in a final difference Fourier synthesis with reasonable Os−H bond distance and was constrained to ride on the Os atom. The largest difference peak and hole 2.253/−0.826 e Å^{-3} are in the vicinity of the Os atom. Further details are given in Table 1.

Computational Details. In the calculations, the PPh_3 ligand has been modeled using a PH_3 group. Geometry optimizations have been carried out for all stable species (reactant, intermediates, and product) and transition states involved in the two possible reaction paths. All calculations have been carried out at the BLYP level of density functional theory. For C and H atoms the 6-31G standard basis set was used, while Ru, Os, and P were represented by the LANL2DZ effective core potentials,[30] which include a double-ζ basis set to describe the valence electrons explicitly. Additionally, to better describe the electronic properties of both hydride and dihydrogen ligands, polarization functions with $\zeta_p = 0.11$[31] have also been added to the standard basis set for the H atoms of these two ligands. The calculations were performed using the Gaussian 98 program[32] installed on Pentium III personal computers with Linux (Red Hat) operating systems.

Acknowledgment. The authors acknowledge financial support from the Hong Kong Research Grants Council.

Supporting Information Available: Tables of crystallographic details, bond distances and angles, atomic coordinates and equivalent isotropic displace coefficients, and anisotropic displacement coefficients for $OsHCl(NBD)(PPh_3)_2$. The material is available free of charge via the Internet at http://pubs.acs.org.

OM000369X

(28) Sheldrick, G. M. *SADABS*, Empirical Absorption Correction Program; University of Göttingen: Germany, 1996.

(29) *SHELXTL Reference Manual* (Version 5.1); Bruker Analytical X-Ray Systems Inc.: Madison, WI, 1997.

(30) Hay, P. J.; Wadt, W. R. *J. Chem. Phys.* **1985**, *82*, 299.

(31) Huzinaga, S. *Gaussian Basis Sets for Molecular Calculations*; Elsevier Science Pub. Co.: Amsterdam, 1984.

(32) Frisch, M. J.; Trucks, G. W.; Schlegel, H. B.; Scuseria, G. E.; Robb, M. A.; Cheeseman, J. R.; Zakrzewski, V. G.; Montgomery, J. A., Jr.; Stratmann, R. E.; Burant, J. C.; Dapprich, S.; Millam, J. M.; Daniels, A. D.; Kudin, K. N.; Strain, M. C.; Farkas, O.; Tomasi, J.; Barone, V.; Cossi, M.; Cammi, R.; Mennucci, B.; Pomelli, C.; Adamo, C.; Clifford, S.; Ochterski, J.; Petersson, G. A.; Ayala, P. Y.; Cui, Q.; Morokuma, K.; Malick, D. K.; Rabuck, A. D.; Raghavachari, K.; Foresman, J. B.; Cioslowski, J.; Ortiz, J. V.; Stefanov, B. B.; Liu, G.; Liashenko, A.; Piskorz, P.; Komaromi, I.; Gomperts, R.; Martin, R. L.; Fox, D. J.; Keith, T.; Al-Laham, M. A.; Peng, C. Y.; Nanayakkara, A.; Gonzalez, C.; Challacombe, M.; Gill, P. M. W.; Johnson, B. G.; Chen, W.; Wong, M. W.; Andres, J. L.; Head-Gordon, M.; Replogle, E. S.; Pople, J. A. *Gaussian 98* (Revision A.7); Gaussian, Inc.: Pittsburgh, PA, 1998.